Ultramicroscopy 000 (2017) 1–10

Contents lists available at ScienceDirect

Ultramicroscopy

journal homepage: www.elsevier.com/locate/ultramic

Scattering delocalization and radiation damage in STEM-EELS

R.F. Egerton

Physics Department, University of Alberta, Edmonton T6G 2E1, Canada

ARTICLE INFO

Article history:
Received 21 July 2016
Revised 4 February 2017
Accepted 18 February 2017
Available online xxx

Keywords:
TEM
STEM
EELS
Inelastic scattering
Delocalization
Radiation damage

ABSTRACT

We discuss the delocalization of the inelastic scattering of 60–300 keV electrons in a thin specimen, for energy losses below 50 eV where the delocalization length exceeds atomic dimensions. Analytical expressions are derived for the point spread function (PSF) that describes the radial distribution of this scattering, based on its angular distribution and a dielectric representation of energy loss. We also compute a PSF for energy deposition, which is directly related to the radiolysis damage created by a small-diameter probe. These concepts are used to explain the damage kinetics, measured as a function of probe diameter, in various polymers. We also evaluate a "leapfrog" coarse-scanning procedure as a technique for energy-filtered imaging of a beam-sensitive specimen.

1. Introduction

The purpose of this paper is to develop analytical formulas, based on wave optics and dielectric theory, to describe the spatial extent of inelastic scattering and the resulting energy deposition that leads to radiolysis damage in a beam-sensitive TEM specimen. Measurements indicate that the delocalization distance is a few nm for valence-electron scattering, and tens of nm for dipole-mode vibrational losses, implying that the EELS signal is generated mainly *outside* the electron probe, in the case of the sub-nm probes used for high-resolution STEM. The delocalization formulas will be applied to previous EELS measurement on polymers, to provide an explanation for the apparent reduction in radiation sensitivity with decreasing probe diameter.

Although scattering delocalization limits the spatial resolution of energy-loss spectroscopy and energy-filtered imaging, it can be exploited to minimize radiation damage, as already demonstrated for aloof-beam spectroscopy of vibrational energy losses [1–3]. The aloof mode (electron probe beyond the edge of the specimen) is useful for spectroscopy but it examines limited regions of the specimen (adjacent to the edge) and is largely incapable of measuring the spatial distribution of the energy-loss signal. We will therefore examine the situation for transmission-mode measurements, to see whether scattering delocalization offers the possibility of mapping a low-loss signal with reduced radiation damage.

2. Delocalization of inelastic scattering

TEM images and diffraction patterns arise from the *elastic* scattering of primary electrons by the electrostatic field of atomic nuclei. In a neutral atom, this field terminates on the surrounding atomic electrons and the scattering is localized to subatomic dimensions, allowing atomic-resolution images. The signal used in electron energy-loss spectroscopy (EELS) arises from the *inelastic* scattering by atomic electrons, which can be excited by a primary electron passing some distance away. This electron-electron scattering is therefore delocalized over a region of size $L(E)$, the delocalization length, whose value depends on the energy loss E involved in the scattering.

For valence-electron scattering ($1\,\text{eV} < E < 50\,\text{eV}$), $L(E)$ can be shown to be a few nm by recording the inelastic signal as a STEM probe is scanned across the edge of a specimen [4–8] or a sharp internal boundary [9]. Similar measurements for vibrational losses (0.1–0.5 eV) have given values of several tens of nm [1]. The general situation is illustrated in Fig. 1, which includes $L(E)$ values estimated from various kinds of TEM measurements (filled data points) . The data is scattered (due to experimental error and the different methods, geometry and definitions used) but demonstrates how the delocalization distance is *inversely* related to energy loss.

For core-electron excitation, giving rise to an ionization edge at some hundreds of eV, $L(E)$ has subatomic dimensions but is important for the interpretation of channeling measurements on crystalline specimens [14–20]. This delocalization has been calculated using Bloch-wave or multislice methods [21–30] and is com-

E-mail address: regerton@ualberta.ca

http://dx.doi.org/10.1016/j.ultramic.2017.02.007
0304-3991/

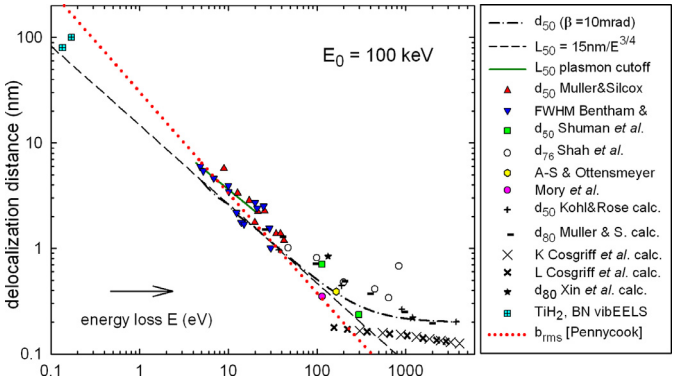

Fig. 1. Delocalization length $L(E)$, adjusted to an incident energy of $E_0 = 100$ keV, based on measurements [1–13] and calculations [24–30]. The dashed line represents Eq. (2) and the dotted red line is based on Eq. (4). (For interpretation of the references to color in this figure legend, the reader is referred to the web version of this article.)

plicated by the influence of elastic scattering, which occurs on a length scale similar to that of the core-loss scattering.

The lines in Fig. 1 are based on relatively simple considerations. For example, we can use the Heisenberg uncertainty principle $\Delta p_x \Delta x \approx h$ to estimate a delocalization distance Δx, taking the momentum uncertainty as $\Delta p_x = \pm(h/\lambda)\theta_{50}$, h being Planck's constant, λ the primary-electron wavelength and θ_{50} the angular width containing 50% of the scattering. Assuming an inverse correlation between impact parameter and scattering angle, the length containing half of the inelastic scattering is:

$$\Delta x \approx h/(2\Delta p_x) \approx 0.5(\lambda/\theta_{50}) \tag{1}$$

Except for Cerenkov and surface-mode losses, inelastic scattering is dominated by a dipole component with a Lorentzian angular distribution of half-width $\theta_E \approx E/2E_0$ but with a cutoff around an angle θ_c, giving $\theta_{50} \approx (\theta_E\theta_c)^{1/2}$. A Bethe-ridge cutoff at $\theta_c \approx (2\theta_E)^{1/2}$ leads to:

$$\Delta x \approx 0.5\lambda/(\theta_E\theta_c)^{1/2} \approx (0.42)\lambda/(\theta_E)^{3/4} \approx (0.71)\lambda(E_0/E)^{3/4} \tag{2}$$

as indicated by the dashed line in Fig. 1. In this figure, the black dash-dot curve represents Eq. (2) combined (by quadrature addition) with the diffraction limit imposed by a 10 mrad spectrometer-collection aperture. The aperture effect is important only for large energy losses; for $E < 50$ eV, $\theta_E < 1$ mrad and almost all the inelastic signal passes through a typical aperture.

Invoking Fourier optics, we can compare the inelastic scattering of electrons with the diffraction of electrons of wavelength λ from a circular aperture of radius a. Observed on a distant screen, the first minimum in the Airy-function intensity corresponds to a deflection angle of $\theta_1 = 0.61\lambda/a$, which forms the basis of the Rayleigh criterion for resolution: $\Delta x = 0.61\lambda/\theta_1$. However, the angular range containing half of the photons is $\theta_{50} = 0.263(\lambda/a)$ and the diameter from which these photons emerge is $d_{50} = (2a)/2^{1/2}$, giving a value:

$$d_{50} \approx 0.37(\lambda/\theta_{50}) \approx (0.53)\lambda(E_0/E)^{3/4} \tag{3}$$

that is slightly smaller than Eq. (1).

Using $\Delta p_x \Delta x \approx h$ and similar arguments, Pennycook [17] obtained an expression for the root-mean-square (RMS) impact parameter b_{RMS} (weighted over the Lorentzian angular distribution) that can also be interpreted as a delocalization length:

$$b_{RMS} \approx (h/2\pi)(v/E)[\log_e(2/\theta_E)] \approx (h/2\pi)(v/E)[\log_e(4E_0/E)] \tag{4}$$

Eq. (4) predicts an energy-loss dependence close to E^{-1} rather than $E^{-3/4}$ but provides an equally good fit to experimental data, as shown in Fig. 1.

3. Point spread function for inelastic scattering

The success of Eq. (3) in predicting delocalization suggests using the methods of Fourier optics to relate the spatial *distribution* of the scattering (here denoted as a point-spread function, PSF) to its angular distribution, easily recorded as an intensity variation at a distant plane (Frauhofer diffraction pattern). In light optics, the PSF is related to the Fourier transform of the angular distribution of scattered intensity *or* scattered amplitude, depending on the lateral coherence length of the illumination [31]. For the *elastic* scattering of electrons, the lateral coherence exceeds atomic dimensions and the object-plane potential is related to the scattered *amplitude* [32,33]. Extending this idea to the inelastic scattering of electrons suggests:

$$\mathrm{PSF(r)} \alpha [FT(\mathrm{d}I/\mathrm{d}\Omega)^{1/2}]^2 \tag{5}$$

where r is an object-plane radial coordinate and FT represents a two-dimensional Fourier transform. Under most conditions, the angular distribution of inelastic intensity is close to a Lorentzian function: $(\mathrm{d}I/\mathrm{d}\Omega) \propto (\theta^2 + \theta_E{}^2)^{-1}$, with an amplitude $(\theta^2 + \theta_E{}^2)^{-1/2}$ whose Fourier transform has a simple analytical form [34], giving:

$$\mathrm{PSF(r)} \alpha [\mathrm{FT}\left(\theta^2 + \theta_E{}^2\right)^{-1/2}]^2 = (k_0 r)^{-2} \exp(-2\theta_E k_0 r) \tag{6}$$

where $k_0 = 2\pi/\lambda$ is the incident-electron wavenumber, making the product $k_0 r$ dimensionless. The exponential behavior at large r is consistent with aloof-EELS measurements of Muller and Silcox [7] The $1/r^2$ dependence at small r agrees with calculations of inner-shell excitation by Ritchie [22] and Wentzel-potential estimates of Rose [21], summing over all energy loss.

Introducing a gradual cutoff of the Lorentzian angular distribution around some large angle (θ_c) makes Eq. (6) more realistic by removing the singularity at $r = 0$, and can be simulated by replacing the $1/r^2$ dependence in Eq. (6) by a Lorentzian function, so that:

$$\mathrm{PSF}(r) \alpha \left(r^2 + r_c{}^2\right)^{-1} \exp(-2\theta_E k_0 r) \tag{7}$$

where $r_c = (2k_0\theta_c)^{-1}$. Fig. 2 indicates that Eq. (7) is a reasonable match to the PSF calculated using Eq. (5).

4. Properties of the inelastic PSF

The inelastic point spread function can be specified more precisely in terms of the probability $(\mathrm{d}^2P/\mathrm{d}E\mathrm{d}V)$ that a primary electron interacts with a volume $\mathrm{d}V$ of specimen, located at a radial distance r from the path of the primary electron and resulting in an energy loss between E and $E + \mathrm{d}E$. Based on Eq. (7):

$$\mathrm{d}^2\mathrm{P}/\mathrm{d}E\mathrm{d}V = C\left(r^2 + b_{\min}{}^2\right)^{-1} \exp(-2r/b_{\max}) \tag{8}$$

where C is an E-dependent coefficient (to be determined) and

$$b_{\max} = 1/(k_0\theta_E) = 1/[(2\pi mv/h)(h\omega/2\pi)/\left(mv^2\right)] = v/\omega \tag{9}$$

The quantity $b_{\max}$ is known as the Bohr adiabatic limit because at larger distances ($r >> b_{\max}$) the electrostatic field induced by the primary electron changes slowly enough to allow atomic electrons to respond adiabatically, without absorbing energy. In fact, the inelastic interaction starts to fall off exponentially at $r \approx b_{\max}/2$, as indicated by Eq. (8). This behavior has been called *dynamical* screening [7] and is directly related to the characteristic angle of the inelastic scattering: $\theta_E = E/(mv^2)$, as seen from Eq. (9).

Please cite this article as: R.F. Egerton, Scattering delocalization and radiation damage in STEM-EELS, Ultramicroscopy (2017), http://dx.doi.org/10.1016/j.ultramic.2017.02.007